The 2010 IEEE/RSJ International Conference on
Intelligent Robots and Systems
October 18-22, 2010, Taipei, Taiwan

Kineto-static Mechanical Synthesis for Nonlinear Property Design of Passive Stiffness using Closed Kinematic Chain

Masafumi Okada and Jun Takeishi

***Abstract*— To prevent the human injury or breakage of the robot caused by interaction or collision with the robot and its environment, it is an important issue to introduce robot softness. However, because not only softness but also stiffness is required for precise task execution, the simultaneous realization of softness and stiffness using time varying stiffness is required in the real environment. We focus on the robot motion, and propose a realization method of time varying stiffness using robot motion and nonlinear passive stiffness. To realize the purpose-designed property of the time dependent stiffness, the nonlinear property of the passive stiffness has to be arbitrary designed considering the robot dynamics. In this paper, we propose the nonlinear property design method of passive stiffness based on kineto-statics with closed kinematic chain. The mechanism is synthesized based on the optimization of the generative force or torque, and purpose-designed stiffness is realized. The proposed method is evaluated by simulations and experiments using the prototype of the landing mechanism.**

I. Introduction

Mechanical softness of robot members or joints is an important issue for safety and adaptation to its environments points of view. As shown in Fig.1, the softness absorbs

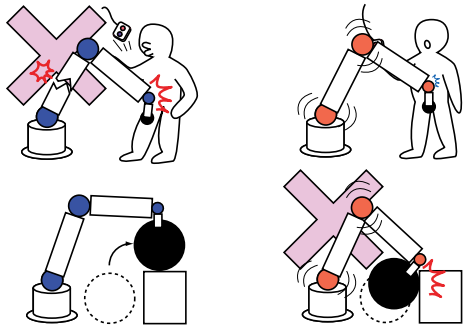

Fig. 1. Impact absorption and task execution with elastic joints

the impact of collision with humans and prevents from a breakage by itself. However, for task execution, stiffness is required for precise control of the robot with a heavy weight. From these considerations, simultaneous realization of stiffness and softness is required, and time variant stiffness or compliance plays an important role. Some researchers have developed variable compliance so far [1].

(1) **Active compliance / Impedance control** realizes a virtual spring and damping by torque and force control of actuators [2]–[5]. This method is effective because an arbitrary characteristic of compliance or viscosity will be realized, however, does not deal with the instantaneous impact force because of a latency of the closed loop bandwidth of control.

(2) **Programmable passive compliance** [6] is realized by additional actuators that change the stiffness of the material. For example, a tendon mechanism with nonlinear spring [7], [8] consists of two redundant actuators that change the internal force of springs. Morita et al. developed Mechanical Impedance Adjuster (MIA) [9]. Wimbock et al. designed a robot hand with variable stiffness [10]. Ham et al. developed MACCEPA for leg compliance [11]. Tonietti and Wolf developed special mechanism for programmable passive compliance [12], [13]. These mechanisms realize an arbitrary compliance however the additional actuator occupies volume and weight of the robot.

On the other hand, passive compliance is a simple way to realize robot softness. It is realized by mechanical softness and has high reliability and robustness, however, low changeability because of its time invariant complaint characteristic.

We focus on that the robot is accompanied by "motion". The landing motion changes the height of the body and the swing motion moves the robot arm to hit a ball, which means the position of the robot p is time variable and assumed to be written by $p = p(t)$. On the other hand, nonlinear stiffness K means the position dependent stiffness which is represented by $K = K(p)$. By connecting "motion" and "nonlinear stiffness", we can realize the time varying stiffness $K = K(p(t))$. Because p is decided by the robot dynamics, $K(p)$ has to be designable to realize an arbitrary property of the time varying stiffness.

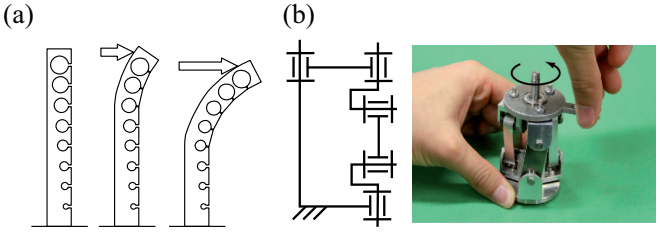

Fig. 2. Nonlinear spring

This research is supported by the "Motion emergence and mutual progression of robot body and intelligence from the dynamical point of view" under Grants-in-Aid for Scientific Research (Category Encouragement of Young Scientists (A)) of Japan Society for the Promotion of Science.

Masafumi Okada and Jun Takeishi are with Dept. of Mechanical Sciences and Engineering, Tokyo TECH, 2 – 12 – 1 Ookayama Meguro-ku Tokyo, JAPAN, okada@mep.titech.ac.jp, takeishi.j.aa@m.titech.ac.jp

So far, some nonlinear stiffness mechanisms have been proposed as shown in Fig.2. Fig.2-(a) is used for a humanoid shoulder mechanism [14] and Fig.2-(b) has high nonlinearity of stiffness based on singularity of the closed kinematic chain [15]. Though these mechanisms realize high nonlinearity of stiffness, they have small design possibility because of the inherent nonlinearity of mechanism. On the other hand, a closed kinematic chain has high nonlinearity of input-output relationship and high design possibility by mechanical synthesis.

The purposes of this paper are as follows.

1) By the combination of "motion" and "nonlinear stiffness", we propose the realization strategy of time varying passive stiffness.
2) To realize the arbitrary property of time varying stiffness, the design method of nonlinear property of the passive stiffness is proposed based on kineto-static mechanical synthesis and closed kinematic chain.
3) The effectiveness of the proposed method is shown by a prototype of the landing mechanism to absorb the impact force.

II. Kineto-static mechanical synthesis for nonlinear stiffness

A. Closed kinematic chain and restoring torque

The stiffness of the closed kinematic chain with a linear spring is designable by changing link parameters. Consider the restoring torque τ of the mechanism (four-bar link system) as shown in figure 3-(a), for example. The link parameters (length of the links and joint angles) are defined in Fig.3-(b). ℓ_i and θ_i mean the length and rotational angle of

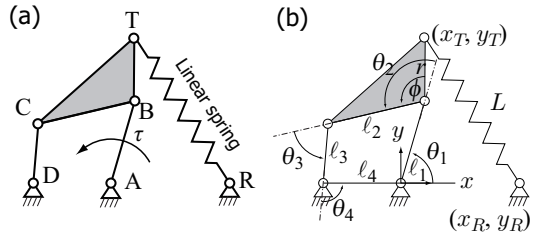

Fig. 3. Closed kinematic chain with four-bar link system and linear spring

link i, r is the length of the one side of the trigonal link and ϕ is its angle. $(x_j,\ y_j)$ $(j = T, R)$ is the position of the edge of the linear spring with the length L. From the kinematics of this mechanism, the following closed loop constraints have to be satisfied.

$$\sum_{i=1}^{4}\theta_i = 2\pi,\ \sum_{i=1}^{4}\ell_i\cos\sum_{j=1}^{i}\theta_j = 0,\ \sum_{i=1}^{4}\ell_i\sin\sum_{j=1}^{i}\theta_j = 0 \tag{1}$$

The natural length of the linear spring is set as L_0, and it yields the initial configuration of the system as follows.

$$L_0 = \sqrt{(x_{T0}-x_R)^2+(y_{T0}-y_R)^2} \tag{2}$$

$$\begin{bmatrix} x_{T0} \\ y_{T0} \end{bmatrix} = \begin{bmatrix} \ell_1\cos\theta_{10} + r\cos(\theta_{10}+\theta_{20}-\phi) \\ \ell_1\sin\theta_{10} + r\sin(\theta_{10}+\theta_{20}-\phi) \end{bmatrix} \tag{3}$$

By defining the potential energy E

$$E = \frac{1}{2}K(L-L_0)^2 \tag{4}$$

that is accumulated to the linear spring with its spring constant K, τ is obtained by

$$\tau = \tau(\theta_1) = -\frac{\partial E}{\partial\theta_1} = -K(L-L_0)\frac{\partial L}{\partial\theta_1} \tag{5}$$

The last term $\partial L/\partial\theta_1$ in equation (5) represents the nonlinearity of the mechanism, and it is obtained by

$$\frac{\partial L}{\partial\theta_1} = \frac{\partial L}{\partial x_T}\frac{\partial x_T}{\partial\theta_1} + \frac{\partial L}{\partial y_T}\frac{\partial y_T}{\partial\theta_1} \tag{6}$$

$$\frac{\partial L}{\partial x_T} = \frac{x_T - x_R}{L},\quad \frac{\partial L}{\partial y_T} = \frac{y_T - y_R}{L} \tag{7}$$

$$\frac{\partial x_T}{\partial\theta_1} = -\ell_1\sin\theta_1 - r\sin(\theta_1+\theta_2-\phi)\left(1+\frac{\partial\theta_2}{\partial\theta_1}\right) \tag{8}$$

$$\frac{\partial y_T}{\partial\theta_1} = \ell_1\cos\theta_1 + r\cos(\theta_1+\theta_2-\phi)\left(1+\frac{\partial\theta_2}{\partial\theta_1}\right) \tag{9}$$

$\partial\theta_2/\partial\theta_1$ is obtained from the partial differential of the closed kinematic constrains in equation (1) with respect to θ_1.

B. Nonlinear property of the stiffness

Based on equation (5), the torque properties are obtained as shown in Fig.4. Two patterns of the link parameters

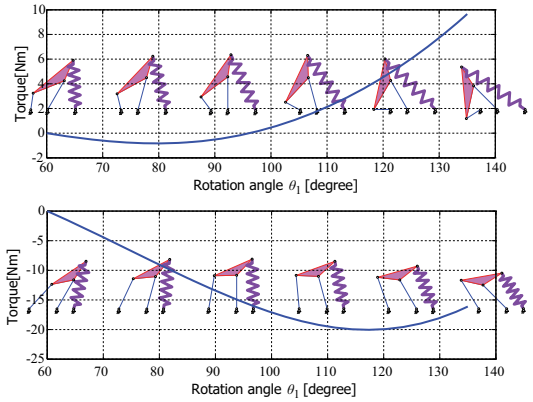

Fig. 4. Torque property of mechanism

are selected. The solid line shows the obtained torque and the link configurations are shown in each joint angle θ_1. These results show that by changing the link parameters, the nonlinear property of the torque or stiffness is changed so much.

C. Kineto-static mechanical synthesis

In this section, nonlinear property design method of the stiffness based on kineto-static mechanical synthesis is illustrated.

Firstly, the reference torque τ_{ref}

$$\tau_{ref} = \left\{\ \tau_{ref}^1(\theta_1^1),\quad \tau_{ref}^2(\theta_1^2),\quad \cdots,\quad \tau_{ref}^N(\theta_1^N)\ \right\} \tag{10}$$

is set with respect to the given joint angle of $\theta_1 = \theta_1^i$ $(i = 1, 2, \cdots, N)$. By setting the objective function J as

$$J = \sum_{i=1}^{N} \left\| \tau_{ref}^i - \tau(\theta_1^i) \right\|^2 \tag{11}$$

the link parameters q_j are optimized by the following gradient method

$$q_j \leftarrow q_j - \frac{\partial J}{\partial q_j}\delta \tag{12}$$

where δ is a small constant. The candidates of q_j are ℓ_i, x_R, y_R, K, r, ϕ and initial value of θ_1.

III. Landing Mechanism with Nonlinear Stiffness

A. Designed mechanism

Applying the kineto-static mechanical synthesis, the landing mechanism is designed. Figure 5 shows the designed passive mechanism which consists of body part and leg part. The leg part consists of two parallelograms that are coupled with 3D kinematic chain (Mechanism g in Fig.5) and yields the vertical motion of foot link (link e – f) as shown in Fig.6. Link parameters in the body part are defined same as

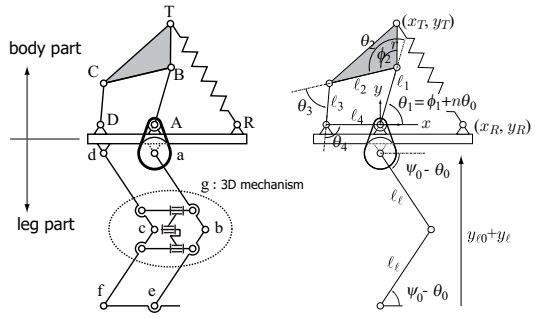

Fig. 5. Designed mechanism

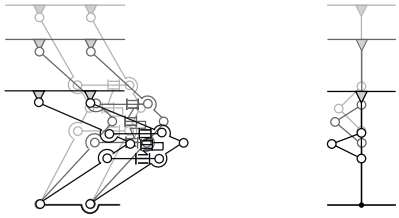

Fig. 6. Motion of leg part

in Fig.3. ϕ_1 is the inital value of θ_1. $\theta_0 = 0$ yields the initial configuration so that the spring becomes natural length. $y_{\ell 0}$ is an initial value of the body height and calculated by;

$$y_{\ell 0} = 2\ell_\ell \sin\psi_0 \tag{13}$$

The motion of this mechanism is shown in Fig.7. The distortion of the body height y_ℓ yields the rotation of θ_0 and it causes the rotation of θ_1 by the timing belt with its gear ratio $1{:}n$. Because of the nonlinearity of the four-bar link, the length of the spring changes with high nonlinearity, which causes the nonlinear ground force of this mechanism.

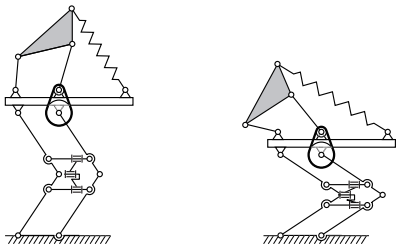

Fig. 7. Motion of the designed mechanism

B. Ground force calculation

According to the change of y_ℓ, the length of the spring is changed and this mechanism yields the ground force F. From the kinematics of the mechanism, θ_0 is calculated as;

$$\theta_0 = \psi_0 - \sin^{-1}\left(\frac{y_{\ell 0} + y_\ell}{2\ell_\ell}\right) \tag{14}$$

The accumulated energy U of the spring is calculated in equation (4), and the ground force F is obtained by;

$$F = \frac{\partial E}{\partial y_\ell} = \frac{\partial E}{\partial \theta_1}\frac{\partial \theta_1}{\partial \theta_0}\frac{\partial \theta_0}{\partial y_\ell} = K(L - L_0)\frac{\partial L}{\partial \theta_1}\frac{\partial \theta_1}{\partial \theta_0}\frac{\partial \theta_0}{\partial y_\ell} \tag{15}$$

From equation (14),

$$\frac{\partial \theta_0}{\partial y_\ell} = \frac{1}{2\ell_\ell \cos(\psi_0 - \theta_0)} \tag{16}$$

is obtained. On the other hand, the rotation angles of the leg part and body part are connected by timing pulley with its gear ration $1 : n$ and

$$\frac{\partial \theta_1}{\partial \theta_0} = n \tag{17}$$

is satisfied. From equations (15), (6) $\sim$ (9), (16) and (17), the ground force is calculated as $F = F(y_\ell)$.

C. Mechanical synthesis of the body part

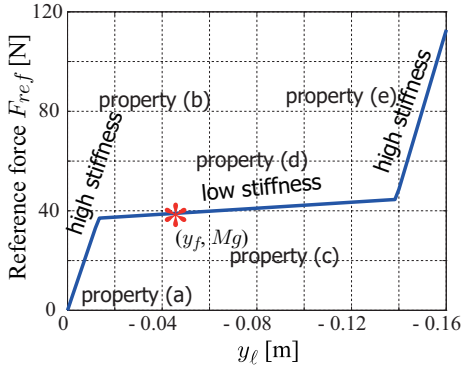

Fig. 8. Reference force that satisfies the given property

1) Set of the reference ground force: By assuming that this mechanism with weight M falls from the height h and collides with the ground with its drop velocity $v_M = \sqrt{2gh}$ with the gravity acceleration g, the properties of the reference ground force F_{ref} are set as follows:

(a) $F_{ref} = 0$ at $y_\ell = 0$ is satisfied because the spring is natural length at $y_\ell = 0$.
(b) The stiffness $K_\ell = \partial F_{ref}/\partial y_\ell$ at $y_\ell = 0$ is sufficiently large. It causes the brake for the drop velocity. We note that the ground force F_{ref} is small even if stiffness is large because of small $|y_\ell|$.
(c) $F_{ref} = Mg$ at $y_\ell = y_f$ is satisfied, where y_f is the final distortion of the height of the body ($t \to \infty$).
(d) The stiffness at $y_\ell = y_f$ is sufficiently small. It does not only contribute to impact absorption but also causes the attenuation of the vibration.
(e) The stiffness in large $|y_\ell|$ is sufficiently large. It plays the role of stopper.

It is not sure that these profile is optimal for impact absorption but come up with kineto-static point of view. Optimization based on biologically inspired method will be required in the future study. From these conditions, the reference ground force F_{ref} is set as shown in Fig.8.

2) Mechanical synthesis: The objective function is set as;

$$J = \sum_i \left\| F^i_{ref} - F(y^i_\ell) \right\|^2 \tag{18}$$

where y^i_ℓ $(i = 1, 2, \cdots, N)$ are the representative points of y_ℓ. The link parameters are optimized so that J is minimized. For simplicity, ψ_0(=75degree), ℓ_ℓ(=20mm), ℓ_4(=10mm) and n(=1.75) are fixed. ψ_0 defines the initial configuration of

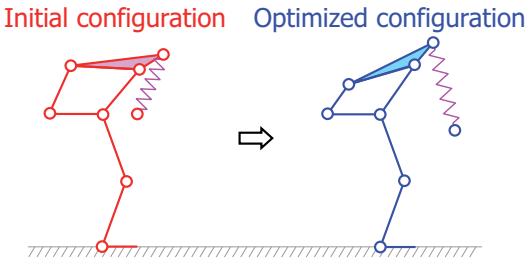

Fig. 9. Initial and optimized configuration

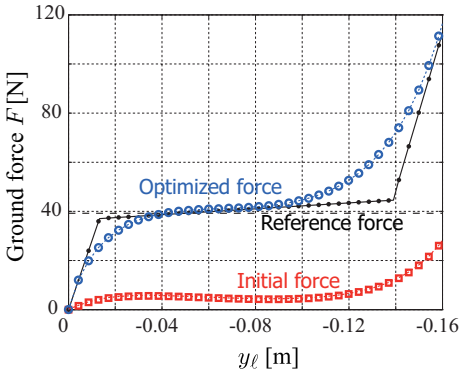

Fig. 10. Obtained ground force

the leg part. The change of ℓ_ℓ and ℓ_4 yields a homologous mechanism. n cannot be taken an arbitrary value because it is decided by the number of teeth of the timing pulley. The design parameters are the following nine parameters: ℓ_1, ℓ_2, ℓ_3, r, ϕ_2 (link parameters of four-bar link), ϕ_1 (initial value of θ_1), x_R, y_R (root position of the spring) and K (spring constant). By setting an appropriate initial value of link parameters, the design parameters are optimized. The initial configuration and the optimized configuration of the mechanism are shown in Fig.9. Figure 10 shows the ground force F of the initial configuration and the optimized configuration.

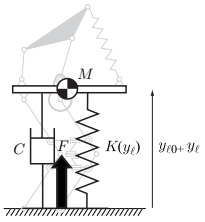

Fig. 11. Model of the mechanism

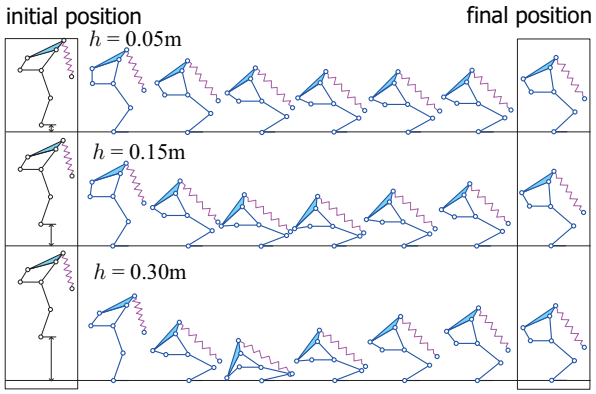

Fig. 12. Landing simulations

IV. Landing Simulation Results

By using the optimized mechanism, the landing simulations are executed, where the dynamics of the inertia terms of members are ignored. The mechanism is approximated by a mass-damper-spring system with the concentrated mass as shown in Fig.11. C is a constant viscous coefficient which is determined from the experimental system in section V and $K(y_\ell)$ is nonlinear stiffness. This mechanism falls from the height $h = 0.05,\ 0.15,\ 0.30$m and collides to the ground with its velocity v_M. The simulation results are shown in Fig.12. The final positions are same because the weight of the robot is same. The transient responses in the simulations are shown in Figs.13 and 14. For comparison, caliculation results of the ground force and body height using a linear spring ($K(y_\ell) =$ const.) are shown. The spring constant is set so that it satisfies $Ky_f = Mg$, which means the final position of the body is same even though linear/nonlinear spring is utilized. Fig.13 shows the ground force. This figure shows that the nonlinear spring reduces the maximum value of the ground force comparing the linear spring (see $h = 0.05$, 0.15m), which means the nonlinear spring works as a soft

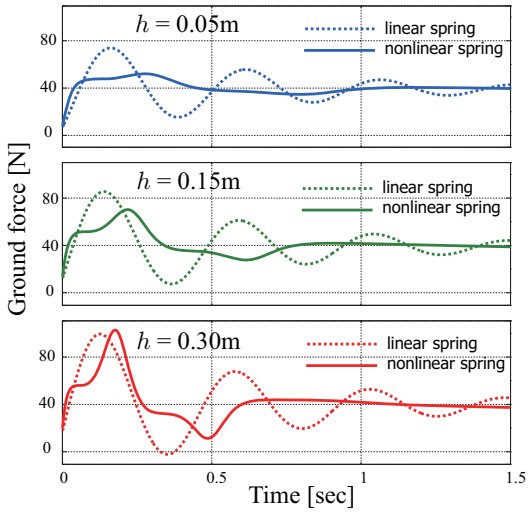

Fig. 13. Simulation results of the ground forces

spring to reduce the impact force. On the other hand, when $h = 0.30$m, even though the maximum ground force of nonlinear spring is larger than linear spring (because of F_{ref} property in (e)), the body height is not so much changed as shown in Fig.14, which means the nonlinear spring works as a hard spring. This is because the nonlinear spring has an advantage of the stopper structure.

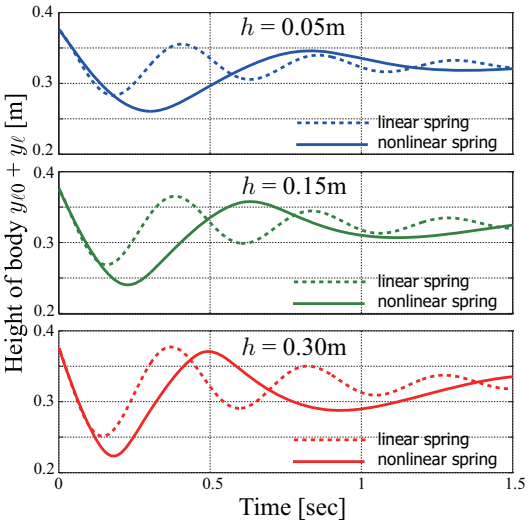

Fig. 14. Simulation results of the height of bodies

V. Prototype of the Proposed Mechanism and Experimental Evaluation

A. Prototype of the mechanism

Fig.15-(a) shows the prototype of the proposed mechanism and (b) shows the 3D closed kinematic constrain of g in Fig.5. The optimized link parameters in section III-C.2 are employed. This mechanism is connected to the linear slider to move vertically and has an encoder and accelerometer to measure the body height and body acceleration.

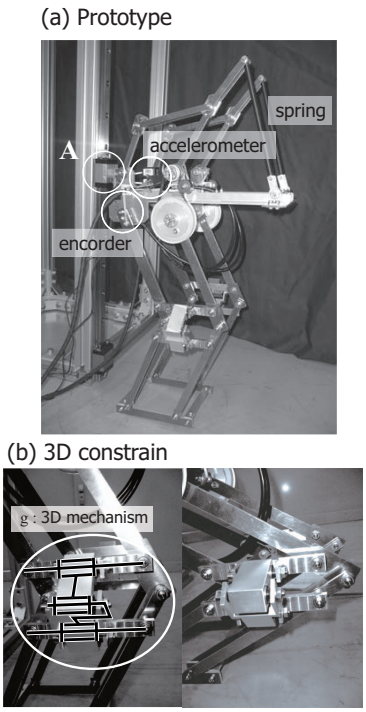

Fig. 15. Prototype of the proposed mechanism

B. Measurement of nonlinear stiffness

The generative ground force of the prototype is measured. By using a weight, the ground force is changed and the height of the body $y_{\ell 0} + y_\ell$ is measured by the encoder. The experimental results are shown in Fig.16. Because of the coulomb friction, y_ℓ is not decided uniquely and the maximum and minimum values of y_ℓ are indicated. The maximum value is shown by red ◯ and minimum value is shown by green □ for the same ground force. The blue line shows the nominal force. After F crosses over 50N, the difference of the nominal value and experimental value tends to be large, this is because the length of the spring transgresses the permissible length of linearity. From these results, the prototype realizes the reference ground force.

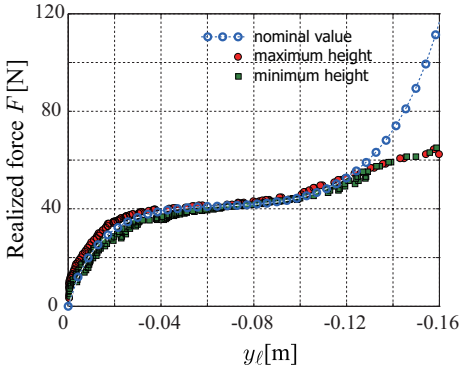

Fig. 16. Ground force of the prototype

C. Landing experiment

By using the prototype, the landing experiment is executed with $h = 0.15$m. The body height $y_{\ell 0} + y_\ell$ is shown in

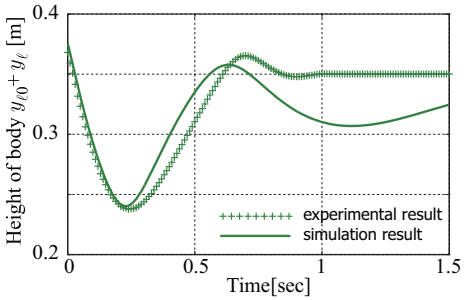

Fig. 17. Experimental result of the height of body

Fig.17. The solid line shows the simulation result (shown in the middle of Fig.14) and "+" shows the experimental results. Because of coulomb friction, the body height of experimental result does not coincide to the simulation result at $t \to \infty$, however, the transient response is similar. And the acceleration of the body is shown in Fig.18, which is obtained from the accelerometer. The solid line shows the

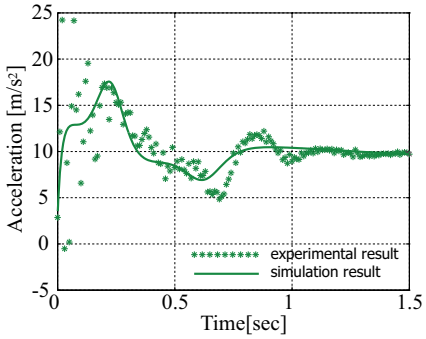

Fig. 18. Experimental result of the acceleration of body

simulation result and "$*$" shows the experimental result. Just after landing, the acceleration of the body is not small, which is because the initial posture of the leg part is close to a singular posture ($\psi_0 = \pi/2$), and the influence of the neglected dynamic term is not small. Some modifications of the initial posture are required. On the other hand, the transient response is similar to the simulation results. From these results, we can see that the proposed mechanism and synthesis method is effective for the impact absorption. The attached movie shows the experimental result.

VI. Conclusions

In this paper, we focus on that the robot motion plus nonlinear stiffness yields time valiant stiffness, and propose a nonlinear property design method of passive stiffness using closed kinematic chain. The results of this paper are as follows;

1) We propose the design method of nonlinear stiffness using a linear spring and nonlinearity of the closed kinematic chain because the link mechanism has large designed possibility by the optimization of the link parameters.
2) The optimization method of the link parameters is proposed to realize the reference ground force based on kineto-statics.
3) To reduce the impact force of landing, the property of the reference ground force is considered and the link parameters are optimized.
4) The effectiveness of the proposed method is evaluated by the landing simulations and experiments using the prototype.

References

[1] R. Van Ham, S. Thomas, B. Vanderborght, K. Hollander, and D.Lefeber. Review of actuators with passive adjustable compliance/controllable stiffness for robotic applications. *IEEE Robotics and Automation Magazine*, SEPTEMBER 2009:81–94, 2009.

[2] R. P. C. Paul and B. Shimano. Compliance and control. In *Proc. of the 1976 Joint Automatic Control Conference*, pages 694–699, 1976.

[3] H. Hanafusa and H. Asada. Stable pretension by a robot hand with elastic fingers. In *Proc. of the 7th International Symposium on Industrial Robots*, pages 361–368, 1977.

[4] J. K. Salisbury. Active stiffness control of a manipulator in cartesian coordinates. In *Proc. of the IEEE Conference on Decision and Control (CDC'80)*, pages 383–388, 1980.

[5] N. Hogan. Impedance control: An approach to manipulation: Part 1∼3. *ASME Journal of Dynamic Systems, Measurement and Control*, 107:1–24, 1985.

[6] K. F. L-Kovitz, J. E. Colgate, and S. D. R. Carnes. Design of components for programmable passive impedance. In *Proc. of IEEE International Conference on Robotics and Automation (ICRA'91)*, pages 1476–1481, 1991.

[7] S. A. Migliore, E. A. Brown, and S. P. DeWeerth. Biologically inspired joint stiffness control. In *Proc. of the 2005 IEEE International Conference on Robotics and Automation (ICRA'05)*, pages 4519–4524, 2005.

[8] K. Koganezawa, T. Inaba, and T. Nakazawa. Stiffness and angle control of antagonistically driven joint. In *Proc. of the 1st IEEE/RAS-EMBS International Conference on Biomedical Robotics and Biomechatronics (BioRob'06)*, pages 1007–1013, 2006.

[9] T. Morita and S. Sugano. Design and development of a new robot joint using a mechanical impedance adjuster. In *Proc. of IEEE International Conference on Robotics and Automation (ICRA'95)*, pages 2469–2475, 1995.

[10] T. Wimbock, C. Ott, A. Albu-Schaffer, A. Kugi, and G. Hirzinger. Impedance control for variable stiffness mechanisms with nonlinear joint coupling. In *Proc. of 2008 IEEE/RSJ International Conference on Intelligent Robots and Systems(IROS'08)*, pages 3796–3803, 2008.

[11] R. Van Ham, B. Vanderborght, M. Van Damme, B. Verrelst, and D. Lefeber. Maccepa, the mechanically adjustable compliance and controllable equilibrium position actuator: Design and implementation in a biped robot. *Robotics and Autonomous System*, 55(10):761–768, 2007.

[12] G. Tonietti, R. Schiavi, and A. Bicchi. Design and control of a variable stiffness actuator for safe and fast physical human/robot interaction. In *Proc. of the 2005 IEEE International Conference on Robotics and Automation (ICRA'05)*, pages 526–531, 2005.

[13] S. Wolf and G. Hirzinger. A new variable stiffness design : Matching requirements of the next robot generation. In *Proc. of the IEEE International Conference on Robotics and Automation (ICRA'08)*, pages 1741–1746, 2008.

[14] M. Okada and Y. Nakamura. Development of the cybernetic shoulder – a three dof mechanism that imitates biological shoulder-motion –. In *Proc. of IEEE/RSJ International Conference on Intelligent Robots and Systems (IROS'99)*, volume 2, pages 543–548, 1999.

[15] M. Okada and S. Kino. Torque transmission mechanism with nonlinear passive stiffness using mechanical singularity. In *Proc. of the IEEE International Conference on Robotics and Automation (ICRA'08)*, pages 1735–1740, 2008.